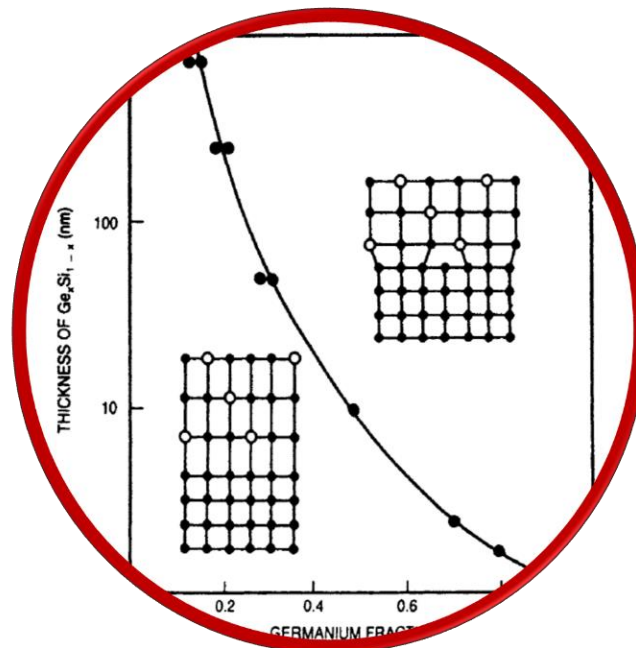


epitaxy



epitaxy application examples

- Wafer scale LEDs

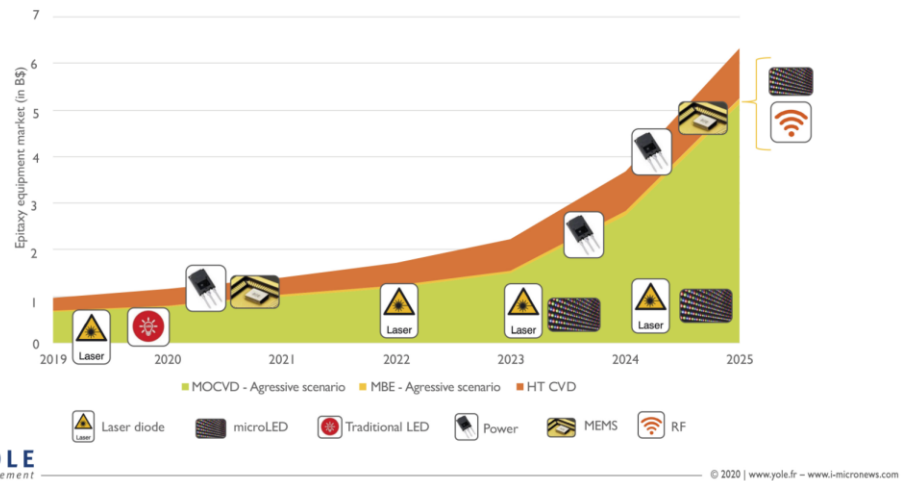


- Laser mouse



Epitaxy equipment market for More than Moore devices: 2019-2025 breakdown by technology

(Source: Epitaxy Growth Equipment for More Than Moore Devices Technology and Market Trends 2020 report, Yole Développement, 2020)



https://www.ledinside.com/news/2019/5/epitaxy_wafer_the_fundamental_phase_microled_display
http://www.yole.fr/iso_album/illus_epitaxy_equipment_materials_equipmentmarket_mtmdevices_yole_jan2020.jpg

content

- Homeepitaxy vs heteroepitaxy
- Crystallography "reloaded"
- Heteroepitaxy notation
- Epitaxial misfit: Strain energy, critical thickness, plastic relaxation
- Elastic relaxation
- Defects in epitaxial films
- Formation of misfit dislocations
- Epitaxy of compound semiconductors
- Design of epitaxial Film substrate combinations
- Liquid phase epitaxy
- ELO - epitaxial overgrowth
- MOCVD
- MBE
- Silicon heteroepitaxy
- Wafer bonding
- Devices and applications

introduction

Two types of epitaxy can be distinguished and each has important scientific and technological implications.

Homoepitaxy refers to the case where the film and substrate are the same material. Epitaxial (epi) Si deposited on Si wafers is the most significant example of homoepitaxy. In fact, one of the first steps in the fabrication of integrated circuit transistors in the past was CVD vapor-phase epitaxy of Si on Si. The reader may well ask why the underlying Si wafer is insufficient; why must single-crystal Si be extended by means of the epi-film layer? The reason is that the **epilayer is generally freer of defects, is purer than the wafer substrate, and can be doped independently of it.**

The second type of epitaxy is known as **heteroepitaxy** and refers to the case where **films and substrates are composed of different materials**, e.g., AlAs deposited on GaAs. Heteroepitaxy is the more common phenomenon. Optoelectronic devices such as light-emitting diodes (LEDs) and lasers utilizing compound semiconductors, are based on heteroepitaxial film structures.

Basic crystal structures and important planes

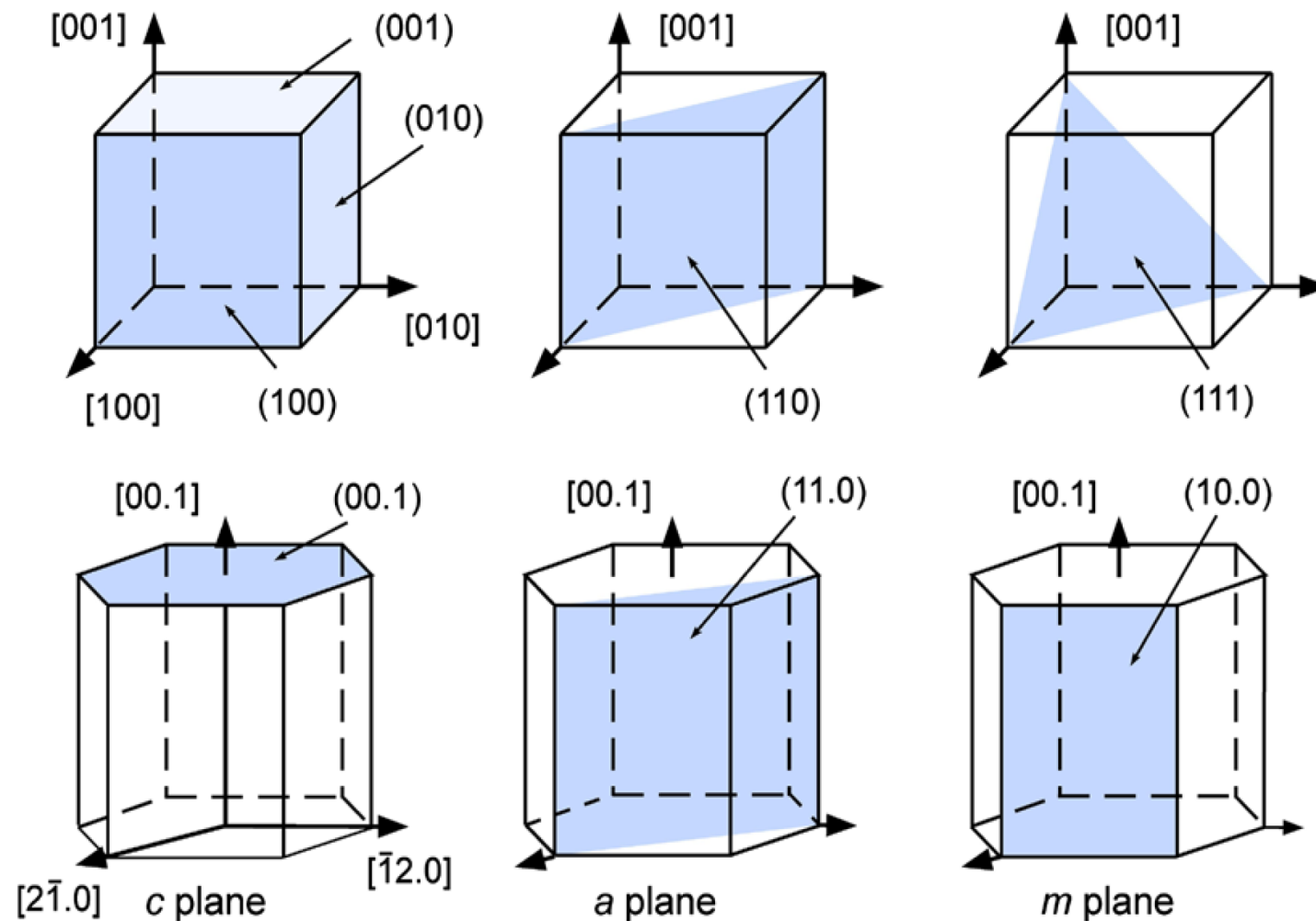


Fig. 2.1 Position of important planes and their Miller indices for cubic and hexagonal lattices

Wafer flats (up to 4 inch)

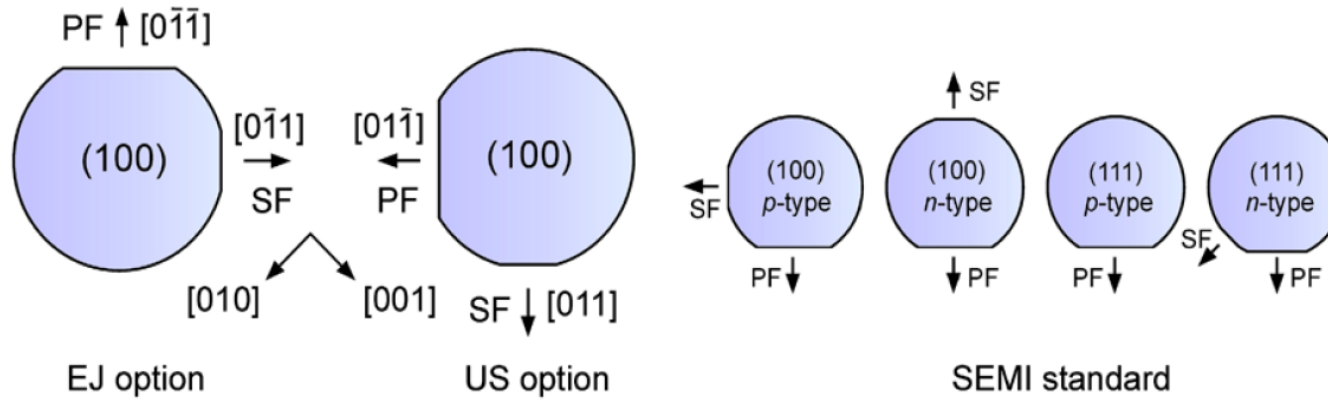


Fig. 2.2 Semiconductor wafers with standard flat orientations according various options. *PF* and *SF* denote primary and secondary flats, respectively. The *arrows* along $[010]$ and $[001]$ refer to the coordinate system of the two wafers on the *left hand side*

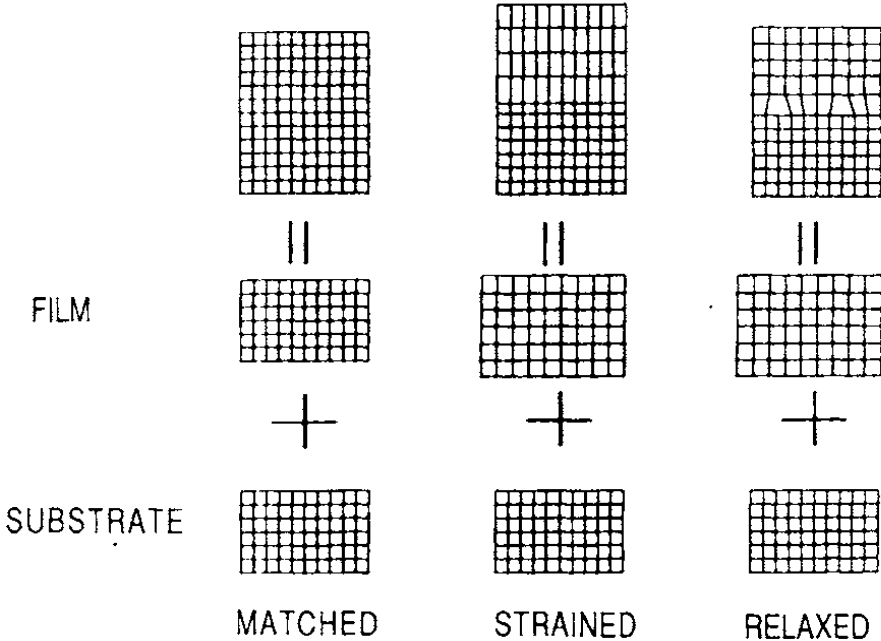
Semiconductor wafers with standard flat orientations. *PF* and *SF* denote primary and secondary flats, respectively. The *arrows* along $[010]$ and $[001]$ refer to the coordinate system of the two wafers on the *left hand side*.

Homoepitaxy vers heteroepitaxy

1) If the **lattice mismatch is zero or very small**, then the heterojunction interfacial structure is essentially like that for homoepitaxy.

2) the two **lattices strain to accommodate their crystallographic differences**

3) **dislocation defects form at the interface (relaxed epitaxy).**



Heteroepitaxy - notation

The indices of the **overgrowth plane** are written as **(HKL)** while those of the **parallel substrate plane** at the common interface are taken as **(hkl)**. The corresponding parallel directions in the overgrowth and substrate planes, denoted by **[UVW]** and **[uvw]**, respectively, must also be specified.

This tetrad of indices, written by convention serves to define the epitaxial geometry.

As an example, **for parallel epitaxy of Ni on Cu**, the notation would read

$(001)\text{Ni} // (001)\text{Cu}$;
 $[100]\text{Ni} // [100]\text{Cu}$.

In this case **both planes and directions coincide**.

For the example

$(\text{III})\text{PbTe} // (\text{III})\text{MgAl}_2\text{O}_4$; $[211]\text{PbTe} // [101]\text{MgAl}_2\text{O}_4$

The **interfacial plane is common but the directions are not**.

Metal/semiconductor heteroepitaxy

A sharp, defect-free interface between cobalt silicide (CoSi_2) and Si can be obtained. Similar epitaxial relationships hold between NiSi_2 and Si.

Both silicides have cubic CaF_2 structures with respective lattice parameters of 5.365 \AA and 5.406 \AA . These are close to the a_0 value for Si, i.e., 5.431 \AA , and therefore, the resulting lattice misfit for CoSi_2 is simply

$$f = (5.431 - 5.365)/5.365 = 0.0123.$$

Other metal silicide films do not exhibit the same epitaxial quality.

Epitaxial misfit I

As described by **van der Merwe** any **epitaxial layer having a lattice-parameter mismatch with the substrate of less than ~9% would grow initially pseudomorphically**. Initially, very thin films strain elastically to have the same interatomic spacing as the substrate, making the **interface coherent** with atoms on either side lining up.

With increasing film thickness the rising total elastic strain energy will eventually **exceed the energy associated with a relaxed structure** consisting of an **array of misfit dislocations**, separated by wide regions of relatively good fit.

At this point the **initially strained film ideally decomposes to this relaxed structure** where a portion of the misfit is relieved by dislocations.

As the film continues to grow, more misfit is relieved until at infinite thickness the elastic strain is totally eliminated.

Epitaxial misfit II

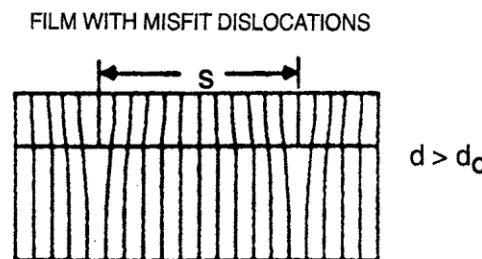
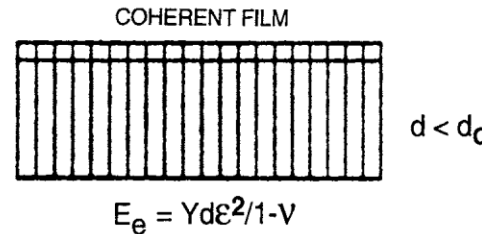
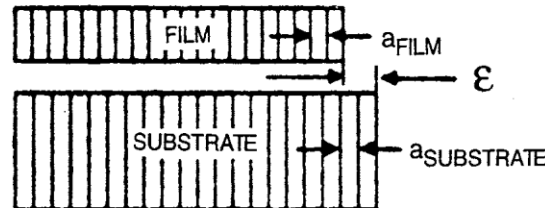
Throughout it is assumed that film and substrate have the same Young's (Y) modulus and same shear μ modulus.

$d < d_c$. In the early stages of film growth, elastic strain energy E_e (per unit area) increases with d as

$$E_e = Y d \varepsilon^2 / (1 - \nu)$$

where ε is the biaxial elastic strain and ν is Poisson's ratio. No dislocations are present in the film.

$d > d_c$. Now consider the formation of (misfit) dislocations at the film-substrate interface as a means of relieving the elastic strain that develops during further film growth. If the dislocations are assumed to be arrayed in a square grid of side S , the elastic strain in the film is reduced from its initial misfit value to $\varepsilon = f - b / S$



Epitaxial misfit III

b/S is proportional to the number of misfit dislocations at the interface and when $b/S=f$ the film strain vanishes.

each dislocation **threads the entire film thickness** and extends the lateral film length by the Burgersvector magnitude, b .

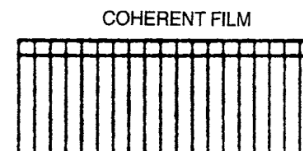
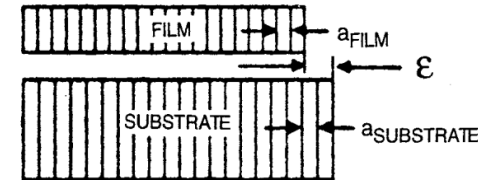
The total strain energy E_T (per unit area) is a sum of the elastic and dislocation energy E_d (per unit area) or

The second term has been derived from the energy per unit length of a dislocation is

$$[\mu b^2/4\pi(1-\nu)] \ln(R_0/b) + E_c,$$

where R_o is a radius about the dislocation where the strain field terminates, and E_c is the dislocation core energy.

Physically the equation indicates that strain energy is a volume energy that increases linearly with film thickness. In contrast, dislocation energy is nearly constant with only a weak logarithmic dependence on d arising from R_o .



$$E_a = Yd\varepsilon^2/1 - V$$

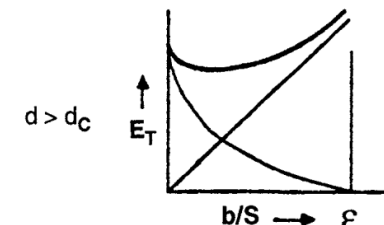
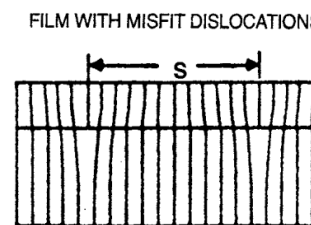
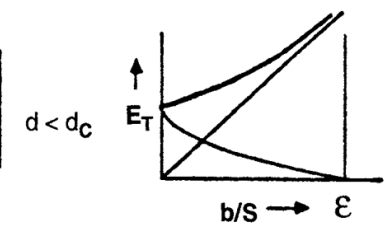


Figure 8-7 Illustration of the Matthews–Blakeslee equilibrium theory of misfit-dislocation formation. (Top) Coherent film is produced when $d < d_c$. (Bottom) Film with misfit dislocations result when $d > d_c$. (From Ref. 18. Reprinted with permission of W. D. Nix.)

Epitaxial misfit IV

The fact that there is a **minimum** in E_T at a **nonzero b/S value** reveals that the structure is in mechanical equilibrium only if dislocations are present.

By minimizing the total energy with respect to dislocation number, i.e., $dE_T/d(b/S) = 0$, and evaluating the resulting expression **at $b/S = 0$** , the critical film thickness (d_c) is

$$d_c = \frac{b}{8\pi(1+\nu)f} \ln(\beta d_c/b),$$

For films thicker than d_c , **misfit dislocations appear**. In the region where d_c is approximately a few thousand angstroms, d_c is roughly $b/2f$.

This means that the film will be pseudomorphic until the accumulated misfit fd_c exceeds about half the unit cell dimension or $b/2$.

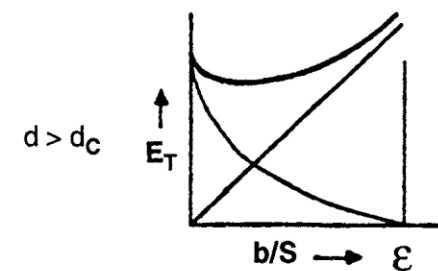
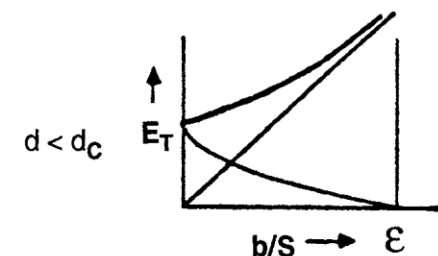
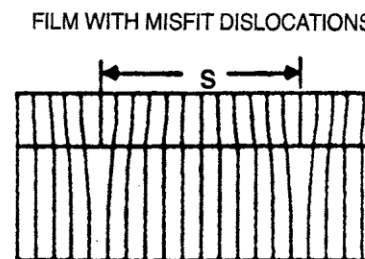
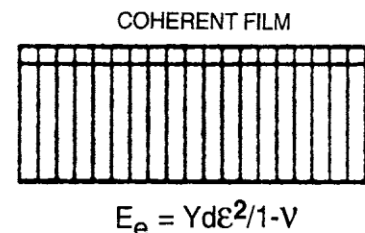
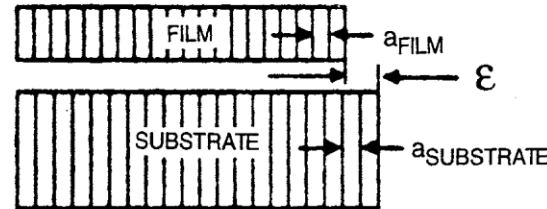


Figure 8-7 Illustration of the Matthews-Blakeslee equilibrium theory of misfit-dislocation formation. (Top) Coherent film is produced when $d < d_c$. (Bottom) Film with misfit dislocations result when $d > d_c$. (From Ref. 18. Reprinted with permission of W. D. Nix.)

Defects in Ge_xSi_{1-x}/Si films

Nature is kinder to us than the Matthews theory would suggest, and considerably thicker films than predicted d_c can be deposited in practice.

The reason is that Ge_xSi_{1-x} strained-layer films are not in equilibrium. Extended dislocation arrays do not form instantaneously with well-defined spacings; rather, dislocations nucleate individually over an area determined by a width w and unit depth, over which atoms above and below the slip plane are displaced by at least $b/2$.

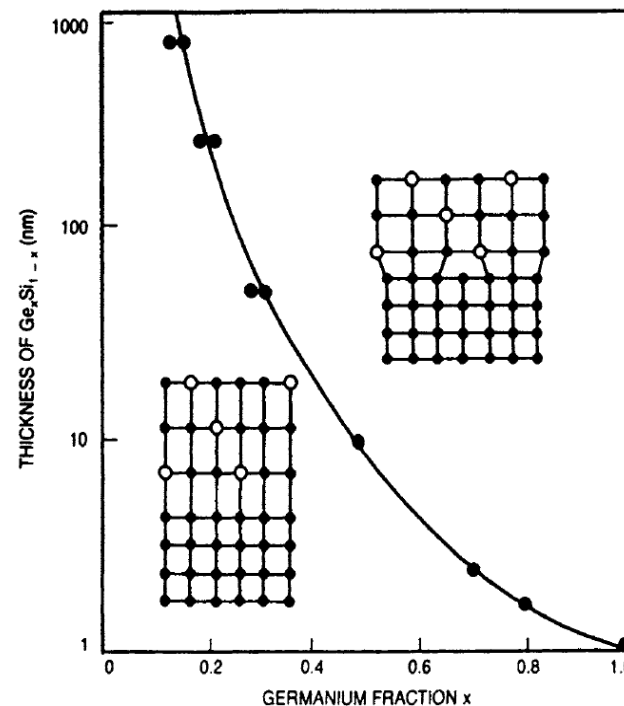


Figure 8-8 Experimentally determined limits for defect-free strained-layer epitaxy of Ge_xSi_{1-x} on Si. Note that f is proportional to Ge fraction. (From Ref. 22.)

Defects in Ge_xSi_{1-x}/Si films II

These films exhibit interesting strain-induced **modulations in surface morphology** that are shown in the TEM cross-sectional image.

The **surface ripples** arise because the film is under compressive stress, a consequence of the fact that lattice parameters of Ge-Si solid-solution alloys necessarily exceed those for Si.

As a result the lattice-plane spacing of the film shrinks near the cusplike troughs and expands at the rounded peaks as schematically depicted.

A flat surface might be expected to represent the minimum energy configuration. However, when **relief of film strain-energy outweighs the tendency of surface energy** to smooth steps arising from the relaxation distortion, roughening of the surface occurs.

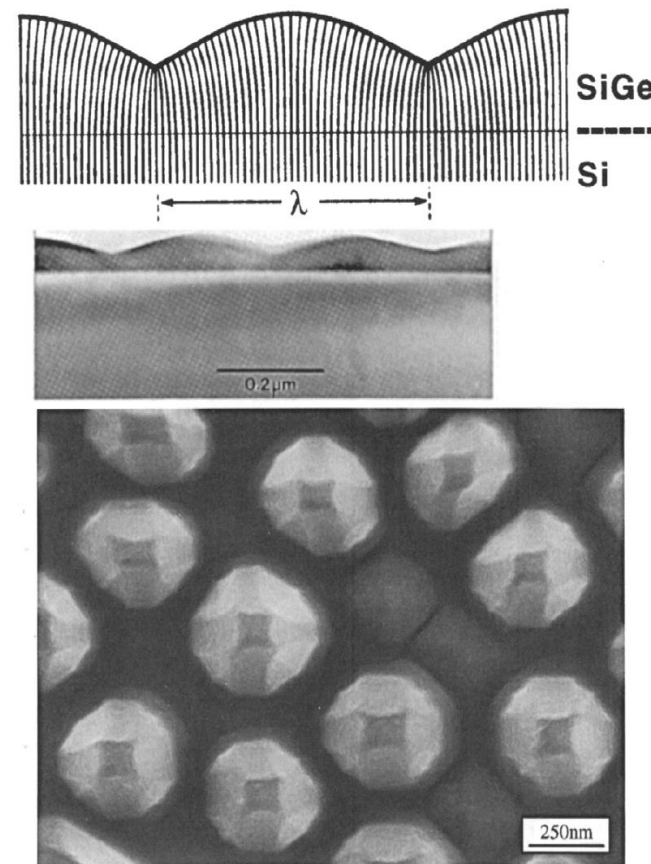


Figure 8-9 (Top) Cross-sectional [100] TEM image of strain-induced surface ripples on an uncapped $Ge_{0.81}Si_{0.19}$ film and accompanying schematic depiction of the distortion of vertical lattice planes. (After Ref. 23. Reprinted with the permission of the author.) (Bottom) Scanning electron micrograph top-view of faceted pyramid and dome-shaped islands formed during growth of a 40 nm thick $Si_{0.7}Ge_{0.3}$ alloy film on (001) Si. Film growth was by UHVCVD (Section 8.6.3.2) at 690°C. The largest islands are 70 nm high. (Courtesy of F. M. Ross, IBM, T. J. Watson Research Center.)

Defects in epitaxial films I

Semiconductor wafers are now largely "dislocation free";

in silicon there are fewer than 10 dislocations/cm²

for GaAs the dislocation density is typically less than 1000/cm².

It is well known that **dislocations, twins, and stacking faults degrade many device properties by lowering carrier concentrations and mobilities.**

They create states in the energy gap and serve to reduce the minority carrier lifetime and quantum efficiency of photonic devices.

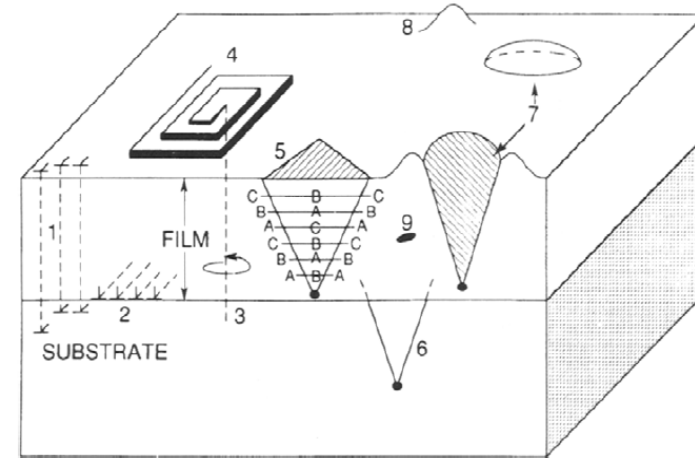


Figure 8-10 Schematic composite of crystal defects in epitaxial films. 1, Threading edge dislocations; 2, interfacial misfit dislocations; 3, threading screw dislocation; 4, growth spiral; 5, stacking fault in film; 6, stacking fault in substrate; 7, oval defect; 8, hillock; 9, precipitate or void.

Defects in epitaxial films II

Defects from the substrate:

- (4) propagation of an **emergent screw dislocation spiral** from the substrate surface into the growing film.
- (5) Stacking faults: **faceted growth hillocks** which nucleate at the film-substrate interface and nest within the epitaxial layer

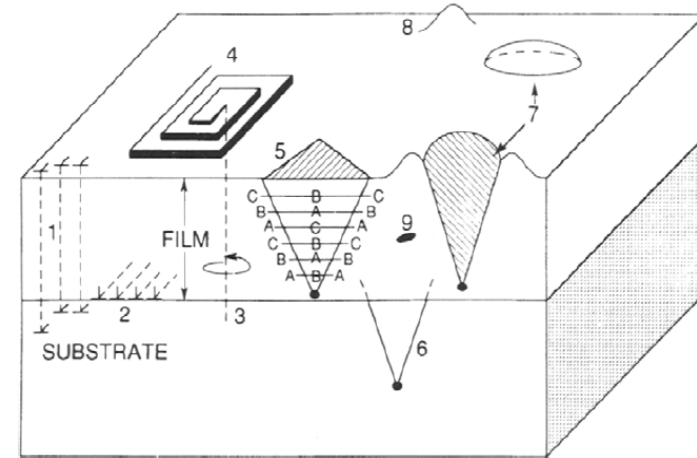


Figure 8-10 Schematic composite of crystal defects in epitaxial films. 1, Threading edge dislocations; 2, interfacial misfit dislocations; 3, threading screw dislocation; 4, growth spiral; 5, stacking fault in film; 6, stacking fault in substrate; 7, oval defect; 8, hillock; 9, precipitate or void.

Formation of misfit dislocations

Although misfit dislocations lie in planes parallel to the substrate-film interface, they generally originate from threading dislocations.

These pierce through the film, the substrate, or both and lie in crystallographic planes that intersect the interface plane.

As it extends into the stressed film the threading component glides or bends in the slip plane. This dislocation segment bends more and more as the film thickens and becomes increasingly stressed.

Correspondingly, the threading dislocation portion in the oppositely stressed substrate moves slightly in the opposite direction. Finally, at the critical thickness $d > d_c$, the film dislocation is able to glide infinitely, leaving behind a stable misfit dislocation at the interface.

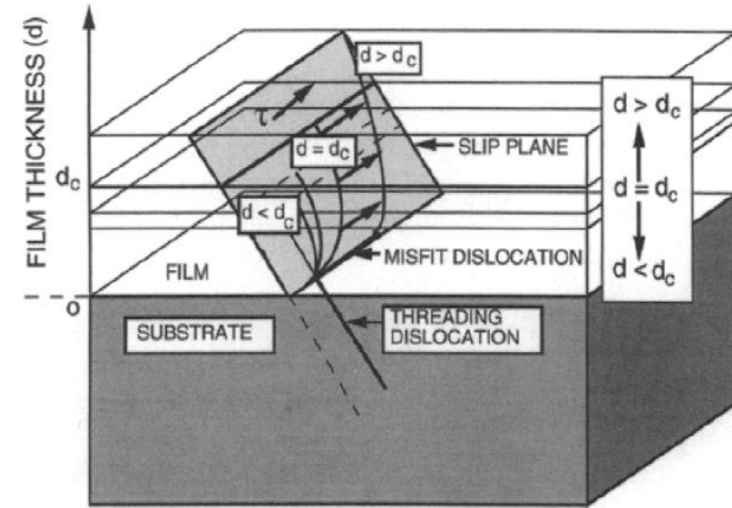


Figure 8-11 A depiction of how stress on thin film plane causes threading dislocation from substrate to form a misfit dislocation when $d > d_c$. (After Refs. 18 and 28.)

Formation of misfit dislocations

Misfit dislocations have been often observed by transmission electron microscopy. For example, a misfit dislocation array, generated during relaxation of a SiGe alloy film on (100) Si.

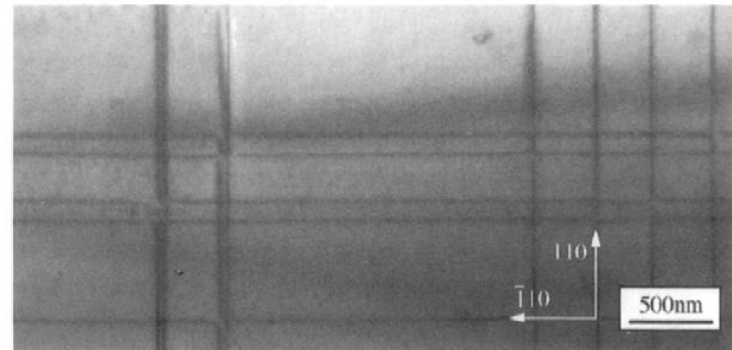


Figure 8-12 Misfit dislocation array generated during relaxation of a 200 nm thick $\text{Si}_{0.85}\text{Ge}_{0.15}$ alloy film on (001) Si. Bright field 220 transmission electron micrograph taken after MBE growth and 700°C annealing. (Courtesy of F. M. Ross, IBM, T. J. Watson Research Center.)

Epitaxy of compound semiconductors

When light is emitted from or absorbed in a semiconductor, **energy as well as momentum must be conserved.**

In a **direct bandgap semiconductor** the carrier transitions between the valence and conduction bands occur without change in momentum of the two states involved.

In the energy momentum or equivalent energy-wave vector, parabola-like (E vs k) representation of semiconductor bands emission of light occurs by a **vertical electron descent from the minimum conduction band energy level to the maximum vacant level in the valence band** (GaAs and InP).

However, in **indirect-bandgap semiconductors** (Ge and Si) the transition occurs with a **change in momentum** that is essentially accommodated by **excitation of lattice vibrations and heating of the lattice**. This makes **direct hole-electron recombination with photon emission unlikely**.

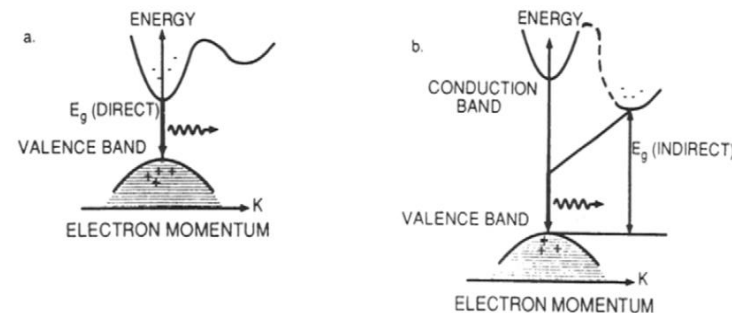


Figure 8-13 Depiction of electron transitions between conduction and valence bands in (a) direct- and (b) indirect-gap semiconductor materials.

Epitaxy of compound semiconductors - bandgap energy

If light of intensity I_0 is incident on a semiconductor surface, the photon intensity at a depth x below the surface is attenuated to $I(x)$,

$$I(x) = I_0 \exp - \alpha x.$$

In all semiconductors α becomes negligible once the wavelength exceeds the cutoff value λ_c . This critical wavelength, is related to the bandgap energy E_g by a variant of the well-known relation $E = hv$ or more simple

$$\lambda_c(\mu\text{m}) = 1.24/E_g(\text{eV}).$$

For direct-bandgap semiconductors the value of α becomes large on the short-wavelength side of λ_c , signifying that light is absorbed very close to the surface. For this reason even thin-film layers of GaAs are adequate, for example, in solar cell applications.

To ensure defect-free interfaces in semiconductor film/substrate heterostructures, it is essential that also the lattice parameters (a_0) of both be closely matched (typically less than 0.1%)

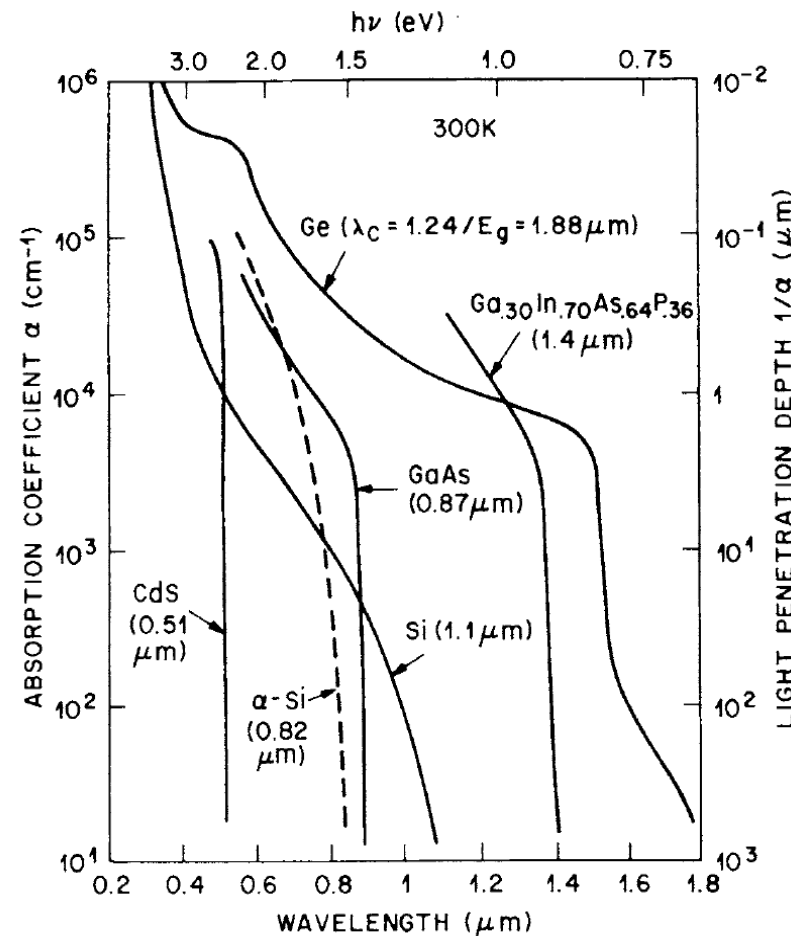
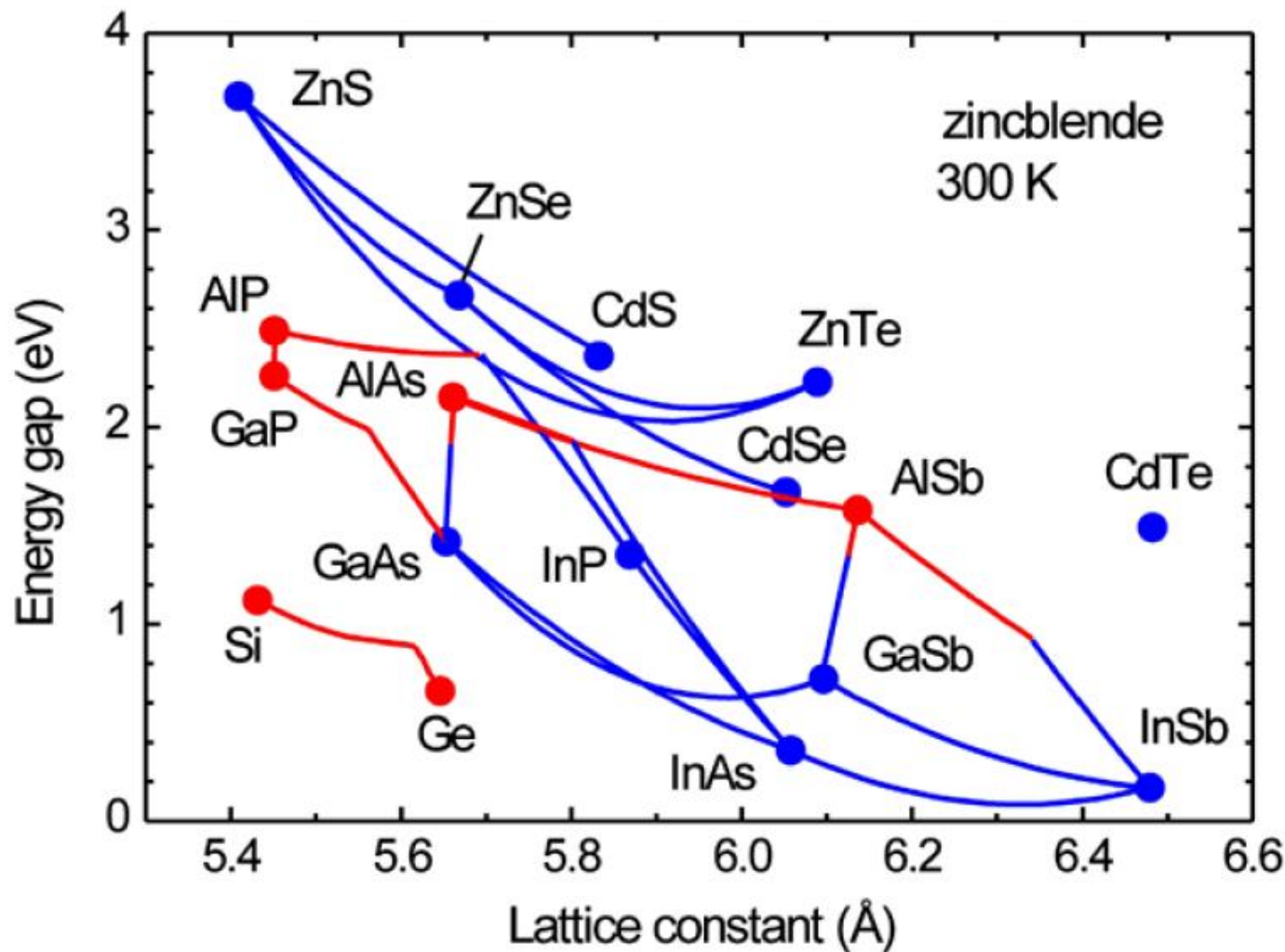


Figure 8-14 Optical absorption coefficients for various semiconductor materials. (Reprinted with permission from J. Wiley & Sons, S. M. Sze, *Semiconductor Devices—Physics and Technology*. McGraw-Hill, New York, 1985.)

Design of Epitaxial Film Substrate combinations

Elements and binary compounds are represented simply as points. Ternary alloys are denoted by lines between constituent binary compounds. Blue and red drawing denotes direct and indirect bandgap, respectively.



Design of Epitaxial Film Substrate combinations

Elements and binary compounds are represented simply as points. Ternary alloys are denoted by lines between constituent binary compounds.

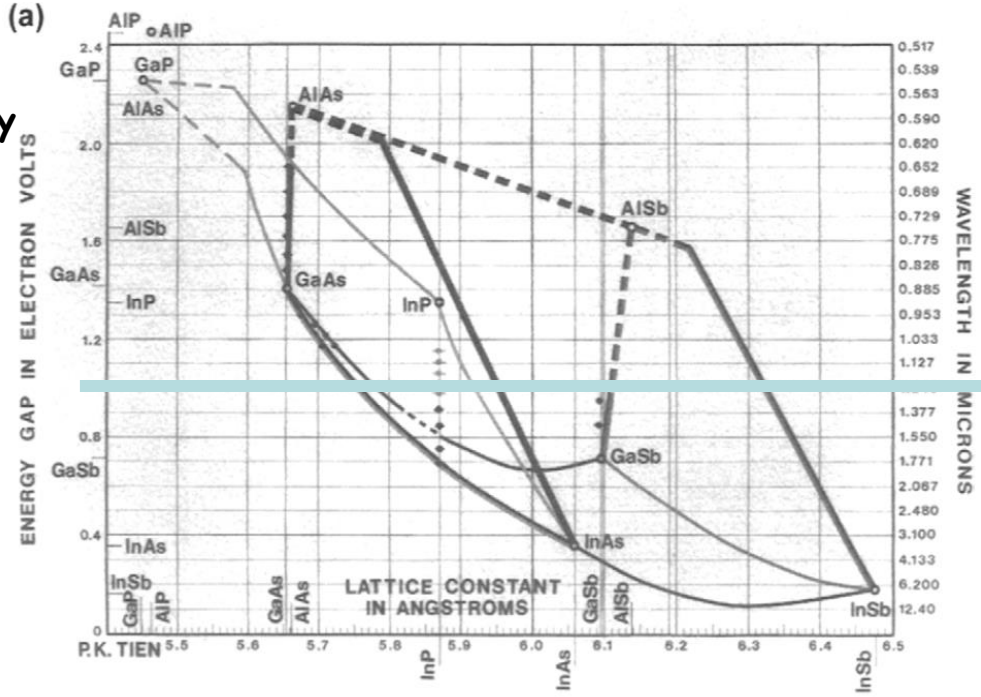
Thus the line between InP and InAs represents the collection of InP_xAs_{1-x} ternary solution alloys. Within the areas outlined by four binary compounds are quaternary alloys.

Solid lines represent direct-bandgap ternary compounds while the dashed lines refer to materials with an indirect bandgap.

Material for optoelectronic device with energy gap of 1.0 eV?

->Extend horizontal line at $Eg = 1.0$ eV we see that the alloys of the following pairs are crossed: GaAs-InAs; GaAs-GaSb; InP-InAs; AlAs-InAs; AlSb-GaSb; and AlSb-InSb.

Although these all appear to be potentially useful, AlSb-GaSb has an indirect bandgap and is disqualified.



Design of Epitaxial Film Substrate combinations

Upon alloying these binary compounds we may assume, in the simplest approximation, that the resultant lattice constants and energy gaps of the ternaries are **weighted averages of the binary values**.

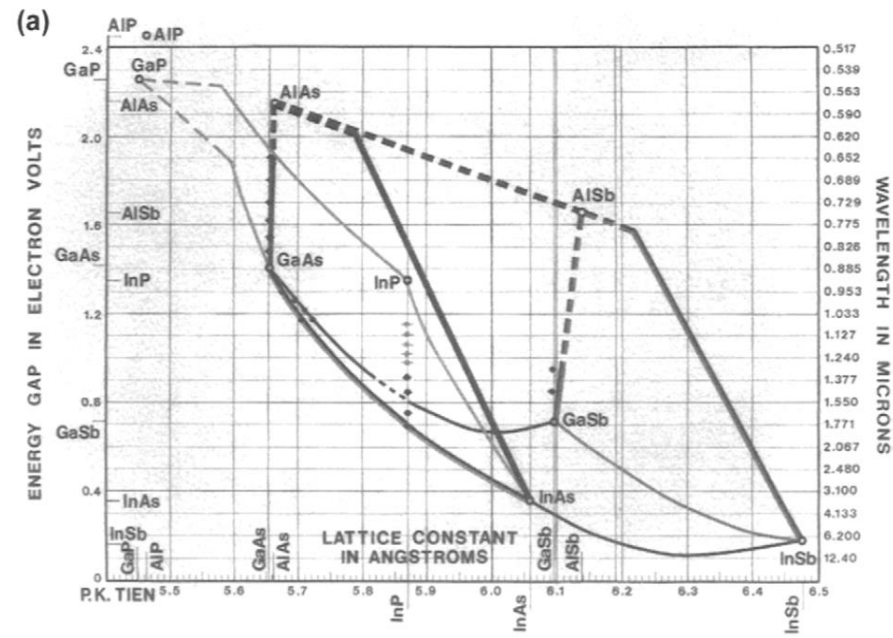
As an example, let us determine the composition of the desired InGaAs alloy for which a_0 must equal 5.76 Å the value at 1.0 eV. For a linear law of lattice-constant mixtures, i.e., **Vegard's law**,

$$a_0(\text{In}_x \text{Ga}_{1-x}\text{As}) = (x) a_0(\text{InAs}) + (1 - x)a_0(\text{GaAs}).$$

Since $5.76 - 6.07x + 5.65(1 - x)$, $x = 0.26$,

and the predicted alloy has the composition $\text{In}_{0.26}\text{Ga}_{0.74}\text{As}$

Next, consider the practical problem of **fabricating lasers emitting coherent light at 1.0 eV**. In these devices, semiconductor films must be deposited on a readily available substrate, e.g., GaAs or InP, and, importantly, be lattice matched to it, which adds another round of alloy design.



Epitaxial films from melts - liquid phase epitaxy

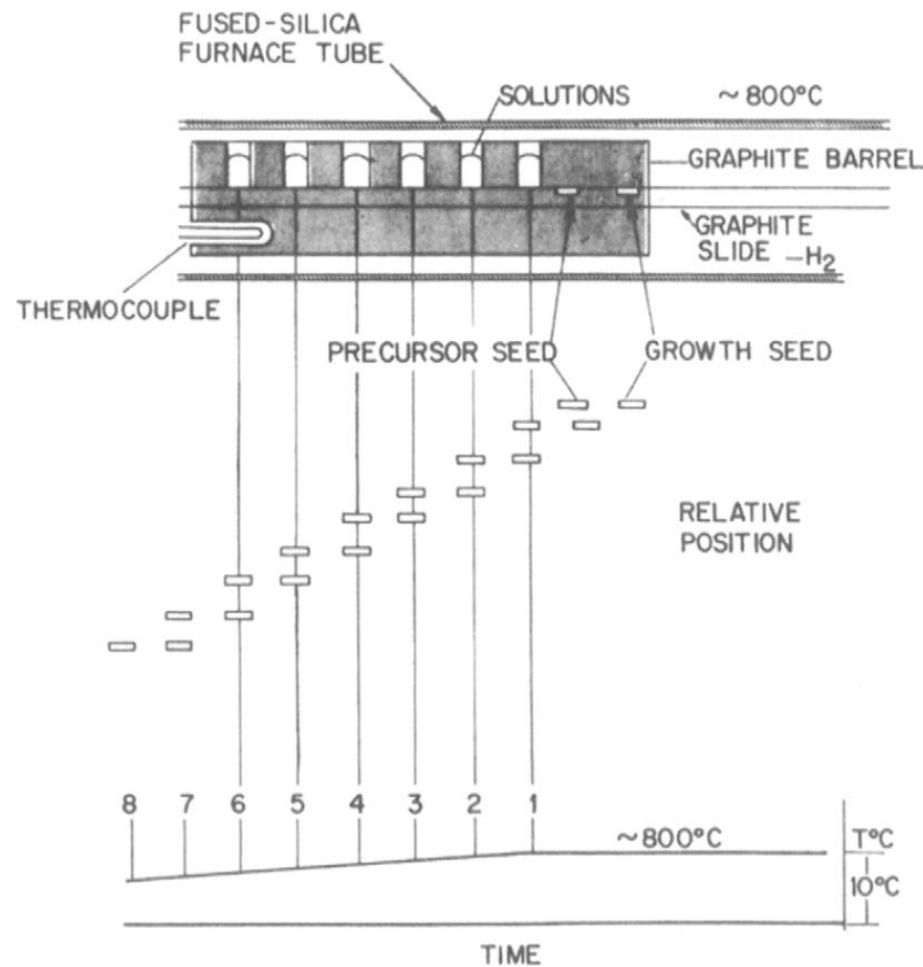
LPE involves the precipitation of a crystalline film from a supersaturated melt onto a substrate.

Consider a Ga-rich melt containing 10 at.% As. When heated above $\sim 920^{\circ}\text{C}$ all of the As dissolves. If the melt is cooled below the liquidus temperature into the two-phase field, it becomes supersaturated with respect to As.

Only a melt of lower than the original As content can now be in equilibrium with GaAs. The excess As is, therefore, rejected from solution in the form of GaAs which grows epitaxially on a suitably placed substrate.

To grow multiple GaAs/AlGaAs heterostructures, the seed substrate is sequentially translated past a series of crucibles holding melts containing various amounts of Ga and As together with such dopants as Zn, Ge, Sn, and Se.

Since growth conditions of LPE processes are close to thermodynamic equilibrium, atoms can efficiently migrate to the growth interface and find energetically optimum positions, which results in a very low density of defects.



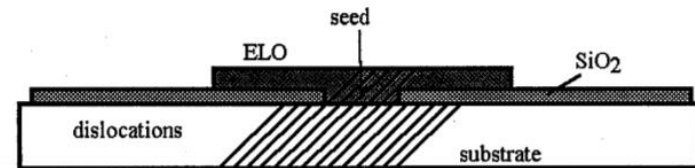
Epitaxial films from melts - lateral overgrowth

Epitaxial lateral overgrowth (ELO) is a method of selective epitaxial growth on partially masked substrates.

Prior to growth the substrate is covered by a thin SiO_2 or Si_3N_4 film which is next patterned by the standard photolithography.

The growth of the ELO layers for instance by LPE starts **selectively in mask-free seeding areas and proceeds laterally over the dielectric film**.

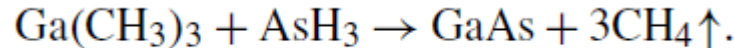
The key advantage of the ELO technique is that **substrate defects can propagate to the layer only through a narrow seed**, and therefore, a defect density in the layer should be considerably reduced.



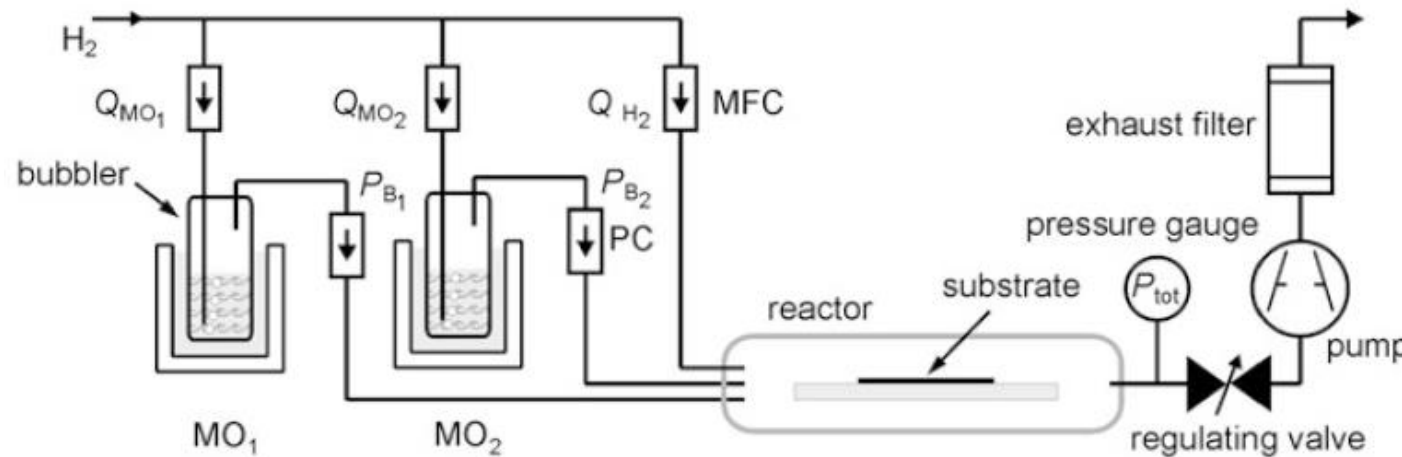
Metalorganic Vapor-Phase Epitaxy

MOCVD was invented to deposit III-V and II-VI compound semiconductor films where it is always the intent to grow **high-quality single-crystal or epitaxial films**. For this reason the acronyms **MOVPE** (metalorganic) or **OMVPE** (organometal) vapor-phase epitaxy or MOCVD are equivalently used when speaking of processes to deposit epitaxial films.

Chemically, precursors largely consist of **metal alkyl compounds** with methyl (M) and ethyl (E) groups present in twofold (di, D) or threefold (tri, T) coordination. A typical net reaction is



Most metalorganic sources are liquids which are stored in bubblers. For transport to the reactor a carrier gas (usually hydrogen) with a flow Q_{MO} is introduced by a dip tube ending near the bottom. Hydrogen is used here as carrier gas and introduced into the metalorganic sources MO_1 and MO_2 . MFC and PC denote mass-flow and pressure controllers, respectively



Metalorganic Vapor-Phase Epitaxy

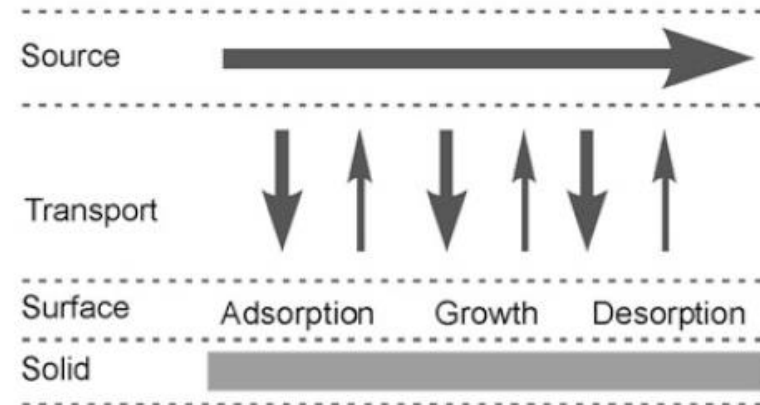
Like all CVD processes the complete treatment of the MOVPE growth process involves numerous gas phase and surface reactions, in addition to hydrodynamic aspects. Such complex studies require a numerical approach.

In a simple CVD picture the reactants in the carrier gas represent the source.

Near the solid surface a vertical diffusive transport component originates from reactions of source molecules and incorporation into the growing layer.

All processes from adsorption at the surface to the incorporation are summarized to interface reactions.

Finally excess reaction products desorb from the interface by diffusion.



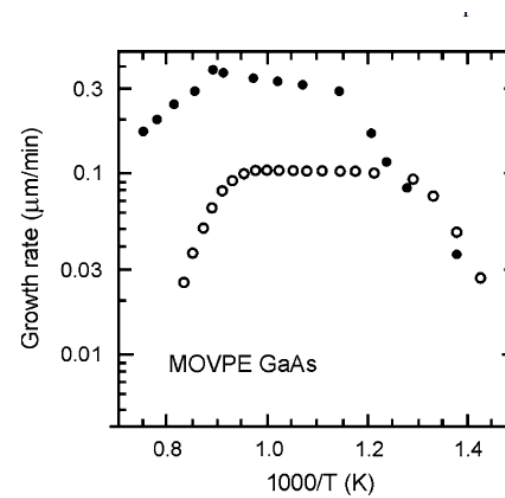
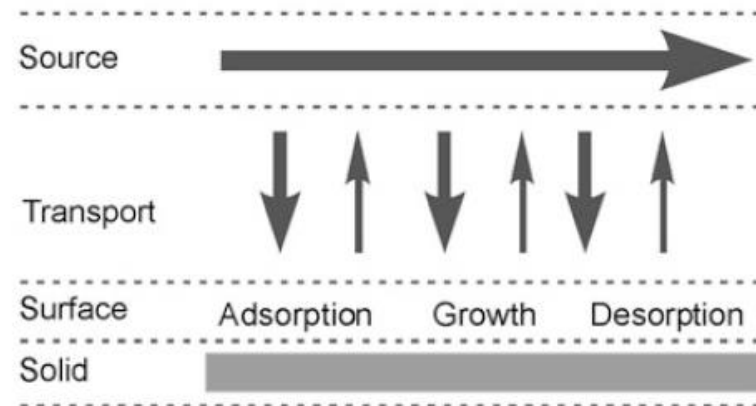
Metalorganic Vapor-Phase Epitaxy

The logarithmic scale of the GaAs growth rate: At low temperature experiment (solid) and simulation (open) show an exponential relation, indicating Precursor decomposition and interface growth reactions lead to a pronounced temperature dependence and is referred to as **kinetically limited growth**.

As the temperature is increased, the growth rate becomes nearly independent on temperature. In this range precursor decomposition and surface reactions are much faster than mass transport from the source to the interface of the growing solid. Since diffusion in the gas phase depends only weakly on temperature, this **process is called transport-limited growth**.

In the high-temperature range growth rates **decrease due to enhanced desorption** and parasitic deposition at the reactor walls, inducing a depletion of the gas phase.

Operation pressures range from 1mbar to atmospheric.



Molecular beam epitaxy

Molecular beam epitaxy essentially involves **highly controlled evaporation** in an ultrahigh vacuum ($\sim 10^{-10}$ mbar) system. The reaction of one or more **evaporated beams of atoms or molecules** with the single-crystal substrate yields the desired epitaxial film.

High-quality film-growth only ensues if **the surface-diffusion-incorporation time (τ_{di}) is less than for the deposition of a monolayer**. If these two times are reversed, unincorporated atoms will be physically buried by the incoming monolayer and give rise to defective layers.

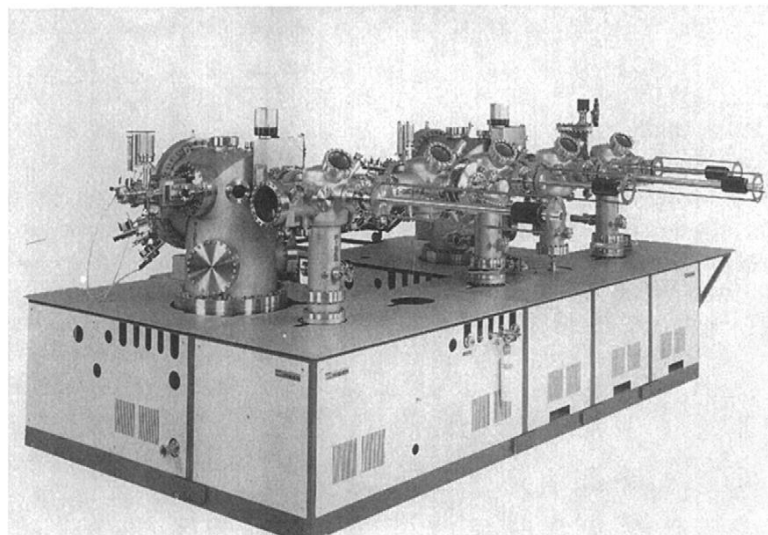
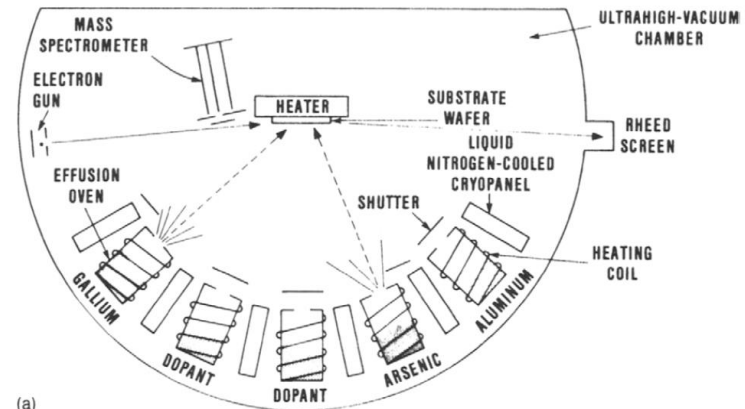
Since τ_{di} is thermally activated, **a low growth temperature limit** is implied for good epitaxy. For example, at typical MBE growth rates in the range of 1 $\mu\text{m}/\text{h}$, excellent quality AlGaAs can be grown at temperatures as low as $\sim 680^\circ\text{C}$ GaAs as low as 475°C and InAs as low as 350°C . In these results it appears that the Group III species governs the growth temperature.

Molecular beam epitaxy

An **MBE system** features independent control of beam sources and film deposition, cleanliness, and real-time structural and chemical characterization capability. In such systems precise fabrication of semiconductor heterostructures from a fraction of a micron thick down to a single monolayer is possible.

Arrayed around the substrate are semiconductor and dopant atom heating sources consisting of **either effusion cells or electron-beam guns**. The latter are employed for the high-melting Si and Ge materials. On the other hand, effusion cells are used to evaporate compound-semiconductor elements and their dopants.

An **effusion cell** is essentially an isothermal cavity containing a hole through which the evaporant exits:



Molecular beam epitaxy

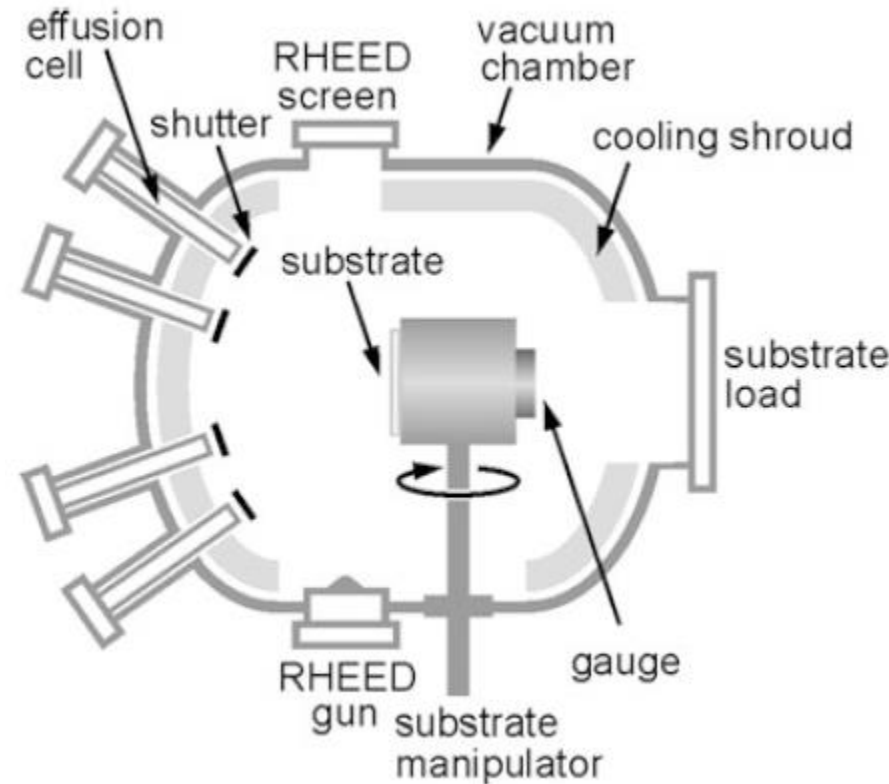
The vacuum is generated in a chamber by pumps and cryoshrouds. Usually effusion cells mounted opposite to the substrate produce beams of different species by evaporation.

The duration of the exposure on the substrate is individually controlled by shutters for a rapid change of material composition or doping.

The substrate is mounted on a heated holder and can be loaded and unloaded under vacuum conditions by a manipulating mechanism. A gauge can be placed at the position of the substrate to measure and calibrate the beam-equivalent pressure (BEP) produced by the individual sources. T

Virtually any MBE system is equipped with an electron-diffraction setup.

Molecular beam epitaxy is performed in ultra high vacuum (UHV), i.e., at a residual-gas pressure below 10^{-9} mbar. The need for such low pressure originates from the required purity of epitaxial semiconductors.

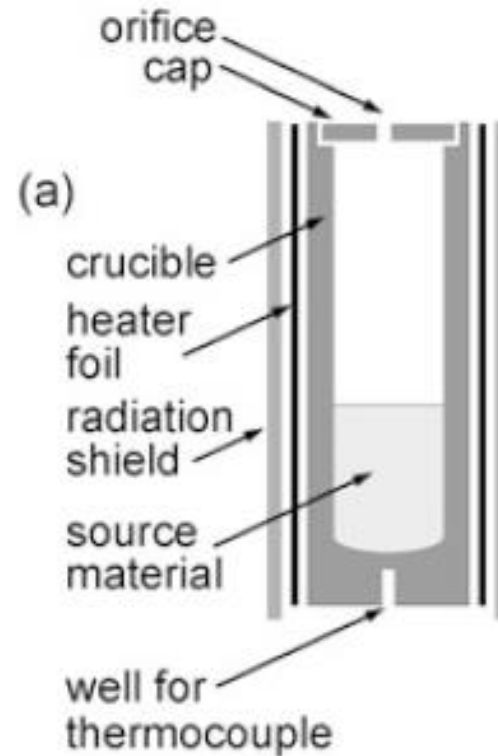


Molecular beam epitaxy - beam sources

For the production of beams from solid or liquid materials usually **Knudsen cells (K-cells)** are employed. They are based on radiative heating and are limited to a maximum temperature of $\sim 1300\text{ }^{\circ}\text{C}$ for **thermal evaporation**. Sources for higher temperatures mostly use **electron-beam evaporation**.

The ideal Knudsen cell is an **isothermal enclosure** which **contains the solid or liquid source material** in thermodynamic equilibrium with its vapor. Effusion occurs through a **small orifice** with an area much smaller than that of the evaporation surface of the source material, and the flux passing this aperture equals the flux of material which leaves the condensed phase to **maintain the equilibrium pressure**.

The ideal Knudsen cell with very thin orifice wall effuses particles with a **cosine angular dependence** like in **classical evaporation**.



Silicon heteroepitaxy

Since the early 1960s Si has been the semiconductor of choice. Its dominance cannot, however, be attributed solely to its electronic properties, for it has mediocre carrier mobilities and only average breakdown voltage and carrier saturation velocities.

The absence of a direct bandgap rules out light emission and severely limits its efficiency as a photodetector. Silicon does, however, possess excellent mechanical and chemical properties. A high modulus of elasticity and high hardness enable Si wafers to withstand the rigors of handling.

Its great natural abundance, ability to be readily purified, possession of a highly inert and passivating oxide, and ease of device processing have all helped to secure a dominant role for Si in solid-state technology.

The idea of combining semiconductors which can be epitaxially grown on low-cost Si wafers is very attractive. Monolithic integration of III-V devices with Si integrated circuits offers the advantages of combined photonic-electronic functionality and higher speed signal processing distributed over larger substrate areas.

application example

Vertical-cavity surface-emitting lasers (VCSELs) are used in fiber communication and are also widely used in computer mice.

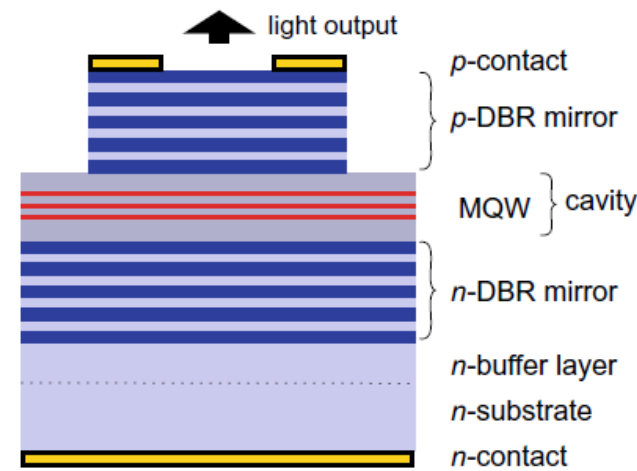
A VCSEL is a semiconductor laser, which emits the radiation vertically via its surface—in contrast to the more common edge-emitting lasers.

Like any laser it consists of an active zone where the light is generated, overlapping with a region where the optical wave is guided.

Light is generated by recombination of electrons and holes which are confined in quantum wells (MQW, multiple quantum well).

The generated photons contribute to the light wave which travels back and forth between two mirrors and a small fraction representing the laser radiation is allowed to emerge from the top mirror. Distributed Bragg reflectors (DBR) are used consisting typically of an GaAs based epitaxial multilayer stack.

VCSEL devices are also fabricated using quantum dots in the active region, formed in the self-organized Stranski-Krastanow growth mode.



Industrial excursion: II-VI lasers in Zürich

Compound Semiconductor Lasers



Material Processing

Automotive

Life Sciences

Military

Communications

Consumer Electronics



II-VI

MATERIALS THAT MATTER® | 28

summary epitaxy

- But, by nature, heteroepitaxial thin films have proven a greater challenge to grow and exploit than bulk crystals.
- Notation: The indices of the overgrowth plane are written as (HKL) while those of the parallel substrate plane at the common interface are taken as (hkl). Note: (HKL)//(hkl); [UVW]//[uvw],
- Pseudomorphic growth with $f < 9\%$.
- Elastic strain energy scales with Elastic modulus * film thickness * strain²
- Strain is relieved by b/S with S dislocation distance and b Burgervector
- For film thickness larger than the critical thickness dislocations appear
- Surface ripples may relax strain energy elastically
- Defects in epitaxial films are dislocations, stacking faults, twin, growth hillocks, etc.
- Misfit dislocations propagate through threading segments through the crystal during the relaxation process
- Epitaxy of compound semiconductors: bandgap engineering through alloying and epitaxial growth on lattice mismatched substrate for defect free growth.
- Liquid phase epitaxy allows to choice of composition along the liquidus line of the phase diagram
- Epitaxial overgrowth limits dislocations to epitaxial window through SiO₂ mask
- MOCVD and MBE: A collection of epitaxial vapor-phase deposition processes based on chemical (CVD, MOCVD) and physical (MBE) methods as well as hybrid combinations (MOMBE, high-vacuum CVD) have been developed.
- An MBE system features semiconductor and dopant atom heating sources consisting of either effusion cells or electron-beam guns. An effusion cell is essentially an isothermal cavity containing a hole through which the evaporant exits. These have enabled extraordinary compositional, structural, and film-thickness control of layered heteroepitaxial structures, resulting in an impressive array of GaAs and InP-based LEDs and lasers for display, recording, and optical communications applications. Ge_xSi_{1-x} materials have also been exploited in high-speed transistors used for assorted computer and communications purposes.

exercises

- Note the indices of the overgrowth planes and directions of Ni/Cu and PbTe//MgAl₂O₄ system.
- How is the film elastic strain calculated in the presence of misfit dislocations.
- What happens if the critical thickness is reached during epitaxial film growth.
- An epitaxial film is deposited with a lattice mismatch of 2% relative to a substrate whose diameter is 10 cm. The epilayer grown at elevated temperature is thick enough that the residual strain is zero. (a) If the Burgers vector is 0.2nm, what is the interfacial misfit-dislocation spacing? (b) A misfit dislocation grid covers the entire film/substrate interface. What is the total length of dislocation line? (c) Estimate the dislocation density.
- Physically explain the ordinate intercepts and curve shapes that lead to E vs b/S variations for $d < d_c$ and $d > d_c$. Plot qualitatively the expected equilibrium misfit dislocation spacing S vs film thickness. In general the experimental misfit dislocation spacing is larger than the equilibrium spacing. Why?
- Compare elastic and plastic relaxation of strained epitaxial layers
- How do misfit dislocations form and how do they relax the film stress
- Describe the overall approach of choosing a material with a required band-gap
- How does epitaxial overgrowth works?
- Describe the LPE process in a few sentences
- What are the basic components of an MBE system?